IOP Publishing Superconductor Science and Technology
Supercond. Sci. Technol. 31 (2018) 095006 (7pp) https://doi.org/10.1088/1361-6668/aad30d

# Multi-core $MgB_2$ wire with a Ti barrier and a reinforced $Al+Al_2O_3$ sheath

**P Kováč[1], I Hušek[1], M Kulich[1], J Kováč[1], T Melišek[1], L Kopera[1] and W Pachla [2]**

[1] Institute of Electrical Engineering, Slovak Academy of Sciences, Dúbravska cesta 9, 841 04 Bratislava, Slovakia
[2] Institute of High Pressure Physics, Polish Academy of Sciences, Sokolowska 29/37, 01-142 Warszawa, Poland

E-mail: Pavol.Kovac@savba.sk

Received 8 June 2018, revised 3 July 2018
Accepted for publication 12 July 2018
Published 1 August 2018

**Abstract**

$MgB_2$ is the lightest superconducting compound, which in connection with lightweight metals like Ti, used for a diffusion barrier and Al, used for an outer sheath, results in a superconducting wire with a noticeably reduced mass compared to traditional wires. Multi-core $MgB_2/Ti/Al+Al_2O_3$ superconducting wire was manufactured by internal magnesium diffusion into a boron process. Basic electrical and mechanical properties of the multi-core wire were studied at low temperatures and compared with a single-core wire and also with GlidCop sheathed multi-core wires. It was found that the lightweight multi-core $MgB_2$ wire exhibited a high critical current density and also a good tolerance to mechanical stresses. This predetermines the potential use of such a superconducting wire for applications where a reduction of the mass of the system is required.

Keywords: multi-core $MgB_2$, reinforced $Al+Al_2O_3$ sheath, critical currents, strain tolerance

(Some figures may appear in colour only in the online journal)

## 1. Introduction

Only a limited number superconducting materials can be used for production of long composite wires. A practical superconductor typically consists of superconducting filaments protected by a diffusion barrier formed inside a conductive and strong metallic sheath. Lightweight superconducting wires are attractive in several areas where the total mass is a crucial issue, like powerful offshore wind turbines, and airborne and space applications [1–4]. Figure 1 shows the specific mass of the most applicable superconducting compounds together with the materials used for the barriers and outer stabilization sheaths. One can see that combining the light metallic sheath materials (Al and Ti) with $MgB_2$ as the superconducting compound would give the superconducting wire a noticeably reduced mass. Some attempts to combine pure Al into composite wires have already been done [5, 6] but without any positive effect.

Although high thermal and electrical conductivity makes pure Al a promising metal for the stabilization of $MgB_2$ superconductors, its low ultimate tensile stress makes it practically unusable as a matrix without any additional mechanical reinforcement. Considering this fact, a much stronger $Al+Al_2O_3$ composite was developed and recently utilized for the outer sheath of single-core $MgB_2$ wires with Ta or Ti barriers [7, 8]. It was shown that the high ductility of the $Al+Al_2O_3$ composite made by powder metallurgy [9] allows the wire to deform by cold rolling or being drawn to high total reductions, without the necessity for intermediate heat treatment [10]. Utilization of the $Al+Al_2O_3$ sheath and Ta barrier was also demonstrated by manufacturing $MgB_2$ wires by cold drawing them into thin wires applicable for a Rutherford $MgB_2$ cable [11]. The mechanical properties and electrical conductivity of the $Al+Al_2O_3$ composite are affected by the initial Al powder purity and particle size [10]. The influence of the initial Al purity and $Al_2O_3$ volume fraction of the $Al+Al_2O_3$ sheath on the thermal and electrical conductivity and mechanical behaviour of single-core $MgB_2$ superconductors protected by Ti barriers was recently studied on three different samples (99.9%–99.999% Al purity and

 

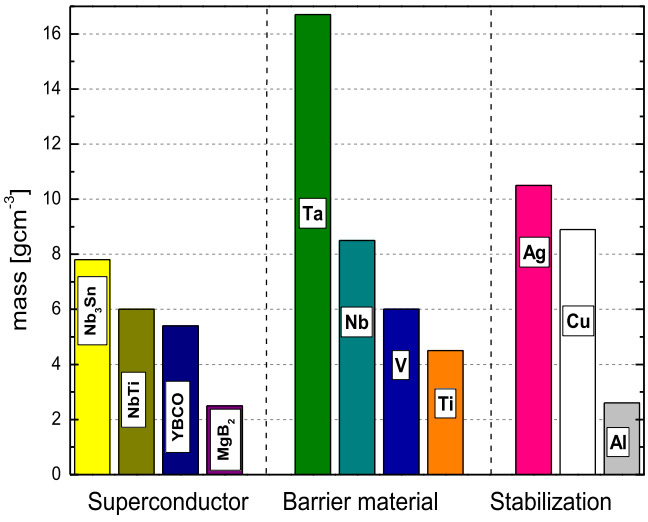


**Figure 1.** Specific weight of the most common superconducting materials, barrier materials and metallic sheaths applicable for outer stabilization.

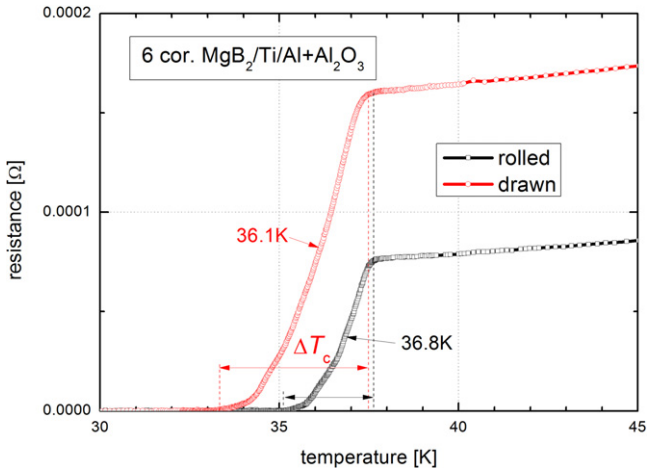


**Figure 2.** Resistive transitions of rolled and drawn wires annealed at 630 °C/15 min.

1.5–3.1 vol% $Al_2O_3$) [12]. It was shown that the critical currents, thermal stability, strain tolerances and Al/Ti interface reactions are influenced by the initial composition of the Al+$Al_2O_3$ sheath.

The aim of this work is to briefly present our newly developed lightweight multi-core wires with Al+$Al_2O_3$ sheaths and $MgB_2$ filaments protected by Ti barriers. Related electrical and electro-mechanical properties are discussed and compared to single-core wires of a similar construction as well as to multi-core wires with GlidCop outer sheets. GlidCop is a copper dispersion strengthened by aluminium oxide made by the internal oxidation technique, which has excellent workability and can be easily deformed by cold drawing or rolling. It has already successfully been used for single- and multi-core $MgB_2$ wires [13–15].

## 2. Experimental

A single-core Mg/B/Ti composite was assembled from a 99.99% pure Mg rod 3.14 mm in diameter, precisely positioned into a central axis of a 99.99% pure Ti tube with a 6.0 mm inner diameter and 8.0 mm outer diameter. The space between the Ti tube and the Mg rod was filled by a 99.8% pure B powder (<1 $\mu$m grain size) in a pure Ar atmosphere. The Mg/B/Ti composite was rotary swaged down to 7.0 mm in diameter, groove rolled to 2.1 mm, again rotary swaged to 1.9 mm and cut into short pieces. Six pieces of the composite wires were inserted into Al+1.5% $Al_2O_3$ tube with dimensions of 6.35/9.05 mm inner/outer diameter together with the central wire made of mechanically stronger Al+3.1% $Al_2O_3$ [10]. The assembled composite was rotary swaged down to a diameter of 7.5 mm and then groove rolled into rectangular wires 1.16 × 1.16 mm and 0.96 × 0.96 mm in dimensions. Additionally, a short piece of the groove rolled wire was drawn down to a diameter of 0.9 mm. Several intermediate heat treatments at 450 °C for 30 min were applied during the deforming process. Prior to the final heat treatment, the as-rolled and as-drawn wire samples were subjected to cold isostatic pressing with the pressure ranging from 0.5–2 GPa. An additional set of the as-rolled samples was subjected to a stepwise tension loading (up to 0.9% tensile strain) applied at room temperature, held for 30 s and then stress was slowly released. All the above described samples were finally heat treated in an Ar atmosphere at 630 °C for 15 min using a fast ramping up (~25 °C min$^{-1}$) and a short peak temperature (with an overshoot by ~19 °C) reaching a maximum at 649 °C. The averaged volume composition of the annealed six-core wires corresponds to 6.9% $MgB_2$ phase, 6.5% holes, 22% Ti barrier, 59% Al+1.6% $Al_2O_3$ outer sheath, plus 5.6% of the central Al+3.1% $Al_2O_3$ core. To study the changes in hardness, HV0.05 micro-indentation hardness testing of selected composite elements was performed after the final heat treatment. The $R(T)$ characteristics of selected wires were measured by a standard four-probe method at a temperature range of 25–300 K using a DC current magnitude of 100 mA. Transport critical currents were measured at the liquid He temperature in external magnetic fields from 3–8 T using a standard DC current transport measurement with a 1 $\mu$V cm$^{-1}$ criterion. In order to better characterize the samples and minimize a self-heating effect at high currents, pulse current measurements at variable temperatures (5–25 K) and fields (1–9 T) were also carried out. The critical current densities were determined from the magnetic loops using Bean's critical state model to establish a relationship between the width of the hysteresis loop $\Delta m$ and the critical current density. Assuming a full penetration of the measured sample by a magnetic field, the particular form of the formula relating $\Delta m$ to $J_c$ can be derived with regard to the current flow geometry. In the case of a cylindrical $MgB_2$ core, the critical current density in a perpendicular field to the wire axis ($B\perp$) is obtained according to $J_c = \frac{3\pi}{4d}\Delta M$, where $\Delta M$ is the width of the hysteresis loop divided by the volume of the $MgB_2$ core, and $d$ is the core diameter. The electro-mechanical characteristics $I_c$ versus tensile strain ($\varepsilon$), stress ($\sigma$) and

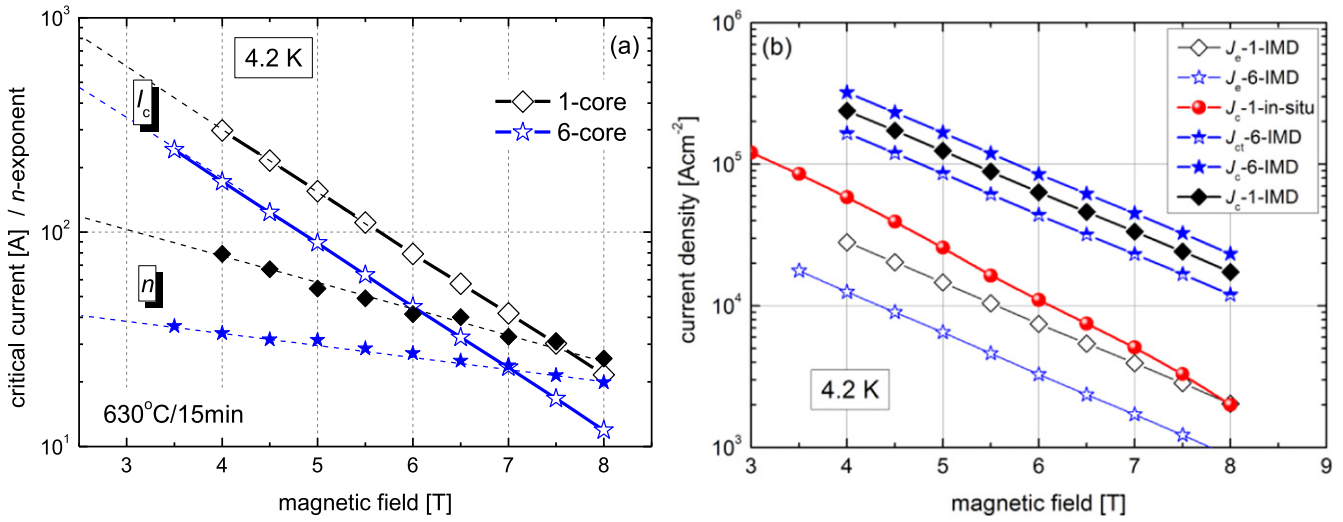


**Figure 3.** Critical currents and $n$-exponents of single- and six-core wire (a) and critical current densities ($J_e$, $J_c$ and $J_{c\text{-true}}$) of the presented six-core wire compared with the $J_c$ of single-core wires made by IMD and *in situ* PIT processes (b).

stress–strain curves $\sigma(\varepsilon)$ were measured at a constant external magnetic field of 6 T.

## 3. Results and discussion

### 3.1. Critical temperature

The critical temperatures of drawn, rolled and differently pressed wires were evaluated from the $R(T)$ characteristics. Figure 2 shows the $R(T)$ of rolled and drawn six-core wires subjected to identical annealing at 630 °C/15 min. One can see that critical temperature $T_c$ (estimated as the middle of the transition) and the transition width $\Delta T_c$ are affected by the applied deformation method. A lower $T_c = 36.1$ K and wider transition $\Delta T_c = 4$ K were measured for the drawn wire having less densified boron in comparison to the rolled one, which has more dense boron resulting in $T_c = 36.8$ K and $\Delta T_c = 2.4$ K. Relatively low $T_c$'s are attributed to the fast ramp and short-time heat treatment held on the temperature the below melting point of magnesium. A noticeably higher critical temperature $T_c = 37.5$ K and narrower $\Delta T_c = 2$ K were measured for the single-core internal magnesium diffusion (IMD) wire with an Al+1.6% $Al_2O_3$ sheath annealed at higher temperatures and longer periods (650 °C/90 min) [13], and also for the wire with a GlidCop sheath ($T_c = 37.2$ K and $\Delta T_c = 2.3$ K) [14]. For the present six-core wire exposed to cold isostatic pressing up to 2 GPa, the $R(T)$ characteristics have shown only a slight, but systematic, decrease in $T_c$ with applied pressure (from 36.8 to 36.6 K in the rolled wire, and from 36.1 to 35.7 K in the drawn one). We observed a similar effect for the GlidCop sheathed multi-core wire subjected to the same pressures, where $T_c = 36.8$ K of unpressed wire was reduced to 36.2 K (by 0.6 K) after 2 GPa isostatic pressing [15]. The $T_c$ decrease by applied isostatic pressure is attributed to a residual strain acting on $MgB_2$ formation, where the residual strain increases with the degree of applied pressure. The smaller $T_c$ reduction (0.2 K) of the 2 GPa pressure-compacted wire with the Al+$Al_2O_3$ sheath compared to the wire with the GlidCop sheath (0.6 K) chould be explained by a smaller residual strain induced inside the softer Al+$Al_2O_3$ sheath.

### 3.2. Critical currents

Figure 3(a) shows the critical currents ($I_c$) and $n$-exponents of a six-core rolled wire with cross-sectional dimensions of 1.16 × 1.16 mm, compared to a single-core one 1.02 × 1.02 mm$^2$ in dimensions [12] which is shown in figure 4. The lower $I_c$ and $n$-exponents of the multi-core wire are attributed to a smaller cross-sectional area of the $MgB_2$ filaments, and also to current redistribution among the non-uniformly reacted filaments. True $J_{ct}$ (for the whole core area) and $J_c$ (for the $MgB_2$ layers) were calculated from the $I_c$ values and the corresponding fill factors of 13.4% and 6.9%, respectively. Figure 3(b) shows the critical current densities: $J_c = 10^5$ A cm$^{-2}$ at 5.75 T, $J_{ct} = 10^5$ A cm$^{-2}$ at 4.75 T for the six-core wire and $J_c = 10^5$ A cm$^{-2}$ at 5.4 T for the single-core one. $J_c = 10^5$ A cm$^{-2}$ of a single-core wire made by a powder-in-tube (PIT) *in situ* process was measured at a considerably lower external field of 3.25 T, and around a one order of magnitude higher $J_c$(8 T) was measured for an IMD wire. Figure 3(b) also shows engineering current densities $J_e = 10^4$ A cm$^{-2}$ at 4.3 T and 5.5 T for the six-core wire and single-core wire, respectively. The $J_e$ values, especially at 4.2 K, are not very high, which is due to non-C-doped $MgB_2$ and also a low filling factor in this first six-core Al sheathed wire. It should be noted that the potential application of light Al+$Al_2O_3$ sheathed $MgB_2$ wire is in temperatures around 20 K where $J_e = 10^4$ A cm$^{-2}$ should be reached at an external field range of 1–3 T (e.g. for powerful wind generators [2], plane engines or some space applications [3]).

Figure 5(a) shows the critical currents of six-core wire measured by three different methods: by direct transport current, by pulse current, and by vibrating sample magnetometer at external magnetic fields of 1–9 T and temperatures

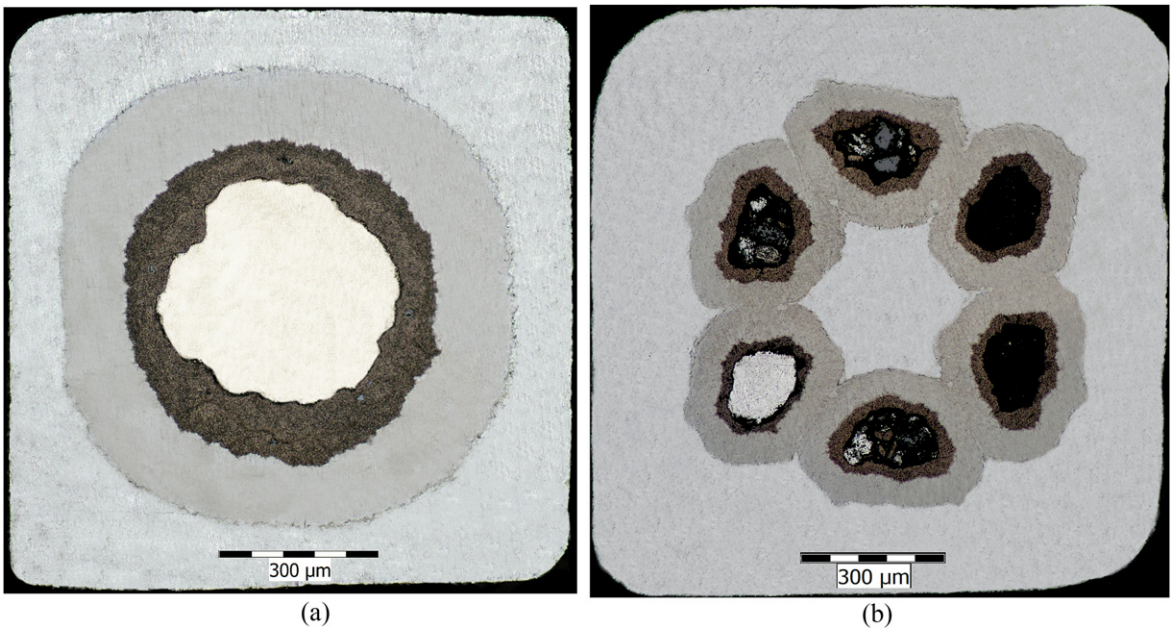


**Figure 4.** Cross-section of the single-core $MgB_2/Ti/Al+Al_2O_3$ wire $1.02 \times 1.02\ mm^2$ in dimensions with 12% $MgB_2$ (a) and the six-core wire $1.16 \times 1.16\ mm^2$ in dimensions with 6.9% $MgB_2$ (b).

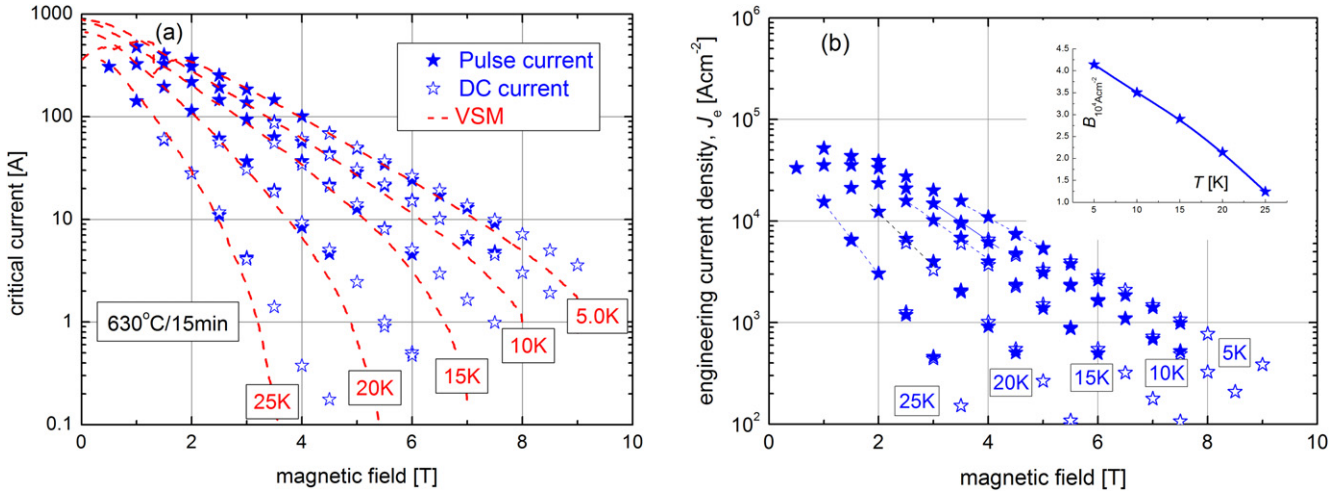


**Figure 5.** Critical currents of six-core $MgB_2/Ti/Al+Al_2O_3$ of $0.96 \times 0.96$ mm wire measured by direct and pulse transport currents at temperatures of 5–25 K together with magnetic ($I_{cm}$) data (a) and corresponding engineering current densities (b).

of 5–25 K. One can see that the magnetic $I_{cm}(B, T)$ values are nearly identical to $I_c$ obtained by DC and pulse current in an external field below 6 T at 4.2 K, and <2.5 T at 25 K.

Deviation of the magnetic $I_{cm}$ curves from the transport curves observed at higher magnetic fields can be explained by the induced current flow combined with a non-identical connectivity in, and across, the core longitudinal axis [16]. On the other hand, figure 5(a) shows a very good relation between the DC and pulse current measurements, which allows us to obtain correct $I_c$ data at low external fields without sample heating. Engineering current densities of the six-core $MgB_2/Ti/Al+Al_2O_3$ wire are plotted in figure 5(b), where the value of $J_e = 10^4$ A cm$^{-2}$ is obtained at a field of 1.3 T for 25 K and at 4 T for 5 K. It should be noted that $J_e(20\ K) \sim 10^4$ A cm$^{-2}$ at an external field of 2 T can be further increased by a more optimal wire design (especially by a higher fill factor).

Because the density of boron powder prior to the final heat treatment is a decisive factor for high critical current densities, the effect of densification by cold isostatic pressing was verified for the present $MgB_2/Ti/Al+Al_2O_3$ wire. Figure 6 shows the evolution of $J_e$ with the pressure applied for rolled and drawn six-core wires, compared with similarly pressed GlidCop and Cu sheathed wires [15]. It is evident that $J_e$ of all wires can be improved by the boron densification, and $J_e$ is affected by the applied deformation and also by the sheath material used. While cold pressing with $p = 2$ GPa improved the $J_e$ of as-drawn wire with an $Al+Al_2O_3$ sheath

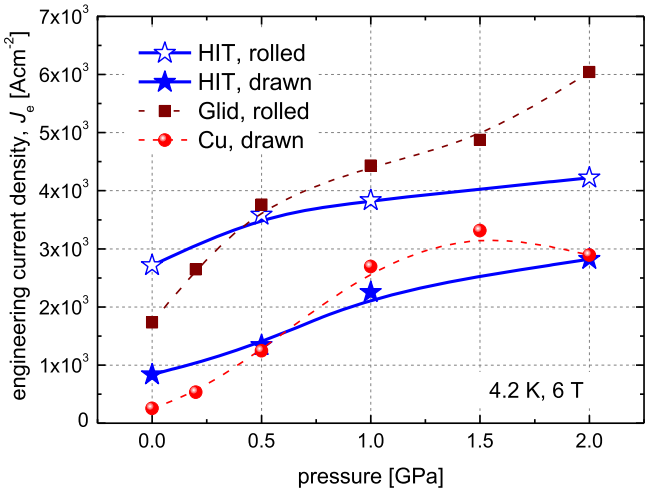


**Figure 6.** Effect of cold isostatic pressing on the engineering current densities of rolled (0.96 × 0.96 mm) and drawn wire 0.9 mm in diameter, both annealed at 630 °C/15 min. The $J_e(p)$ dependences of GlidCop and Cu sheathed multi-core IMD wires are compared.

by 3.38 times, only a 1.55 times $J_e$ improvement was reached for the more dense as-rolled wire densified by the same pressure. The presented results are compared with similar experiments done for multi-core IMD wires in figure 6, where the ratios $J_{e(2GPa)}/J_{e(0)} = 11.4$ and 4.17 have been obtained for Cu and GlidCop outer sheaths, respectively [15].

These results show clearly the positive effect of isostatic pressing on the critical currents in the $MgB_2$ layers, which is a consequence of the improved boron powder density prior to heat treatment. The density improvement was confirmed by micro-hardness measured in the $MgB_2$ filaments formed after drawing (~500 $HV_{0.05}$) and rolling (~800 $HV_{0.05}$) which subsequently, after pressing at 2 GPa, increased to ~950 $HV_{0.05}$ for both pressed wires. The isostatic pressing shows only how the densification of boron powder can affect the final current density, but rolling deformation is a much more practical technique applicable for long conductors.

### 3.3. Effect of mechanical stresses

*3.3.1. Axial tension.* Accurate measurement of the elastic behaviour of a wire is important for understanding of its response to a tensile load. While low axial tension imposed on a superconducting wire may improve the critical current, exceeding a tolerance limit will destroy it. Figure 7(a) shows the stress–strain characteristics measured at 4.2 K for single- and six-core Al+$Al_2O_3$ sheathed wires compared to $\sigma(\varepsilon)$ of a GlidCop sheathed seven-filament wire. Due to the differences between the total volume and quality of the outer sheath materials of both wires, the single-core wire (~50% of Al +1.5 vol% $Al_2O_3$) and six-core wire (59% Al+1.5 vol% $Al_2O_3$ outer sheath with 5.5% Al+3.1 vol% $Al_2O_3$ in the central filament), higher $\sigma(\varepsilon)$ values were measured for the multi-core wire. The strength of the multi-core wire approaches that of the GlidCop sheathed wire, which indicates very good mechanical behaviour. The corresponding effect of tensile strain on the critical current is presented in figure 7(b), where the normalized critical currents measured at an external field of 6 T are plotted versus the tensile strain $\varepsilon$. One can see the identical tendency of critical current increase with $\varepsilon$ for all the presented wires, but different irreversible strain $\varepsilon_{irr}$ values are obtained. While the single-core wire shows the $MgB_2$ breaking at $\varepsilon_{irr} = 0.35\%$ and a corresponding stress of 214 MPa, the six-core wire behaves reversibly up to a strain $\varepsilon_{irr} = 0.55\%$ and stress of 343 MPa (see arrows in figure 7(a)). Surprisingly, the irreversible strain of the GlidCop sheathed wire $\varepsilon_{irr} = 0.48\%$ is lower, in spite of the stronger sheath with an irreversible stress of 357 MPa. This can be explained by a higher volume fraction of the brittle $MgB_2$ structure (~11%), like in the six-core wire (6.9%). It clearly demonstrates that light multi-core $MgB_2$ wires may have comparable strain and stress tolerances to GlidCop sheathed wires, which can be advantageously utilized. The micro-hardness of the outer Al+1.5% $Al_2O_3$ sheath (59% of total conductor area) was 66 $HV_{0.05}$ in comparison to 83 $HV_{0.05}$ measured for the central Al+3.1% $Al_2O_3$ core (5.5% of the total area).

During the winding process in practical react and wind applications, the superconducting wire is subjected to a certain degree of tension load. Therefore, it is advisable to estimate an upper limit of the tension load that can be applied. Figure 8(a) shows the stressing characteristics applied for six-core wire at room temperature. A set of short superconducting wires were subjected to a variable tension load with a maximum strain ($\varepsilon_t$) up to ~0.9%, then the load was released ($\varepsilon_t$ is reduced to $\varepsilon_r$, see arrows in figure 8(a)) and, subsequently, critical currents at 4.2 K were measured. Figure 8(b) shows the normalized critical currents versus the strain ($\varepsilon_t$ or $\varepsilon_r$) applied at room temperature (plotted by circles) which are compared with normalized $I_c$ values for strain $\varepsilon_t$ applied at 4.2 K (plotted by blue stars). The maximum strain $\varepsilon_t$ applied at 300 K to the six-core wire indicates the value of the irreversible level $\varepsilon_{irr} > 0.6\%$. But, in the real case, the critical currents were measured on unloaded samples at strains $\varepsilon_r$. Consequently, the irreversible strain $\varepsilon_{irr} \sim 0.4\%$ is a realistic value for the wire tensioned at room temperature in comparison to $\varepsilon_{irr} = 0.54\%$ obtained at 4.2 K.

Figure 9 compares the effect of tensile stress applied at 300 K and 4.2 K. As visible in the graph, critical currents below the limit of irreversible stress of both temperatures follow the same dependence. It should be noted that each point at 300 K dependence represents one individual stressed and measured sample. Due to temperature-dependent strengthening of the metallic sheath, the irreversible stress of the six-core wire at 4.2 K, $\sigma_{irr(4.2K)} = 343$ MPa, which is comparable to the GlidCop sheathed wire. In addition, the value of $\sigma_{irr(300K)} = 180$ MPa shows that the presented $MgB_2$ wire will not degrade if the manipulation stress will be kept below this level.

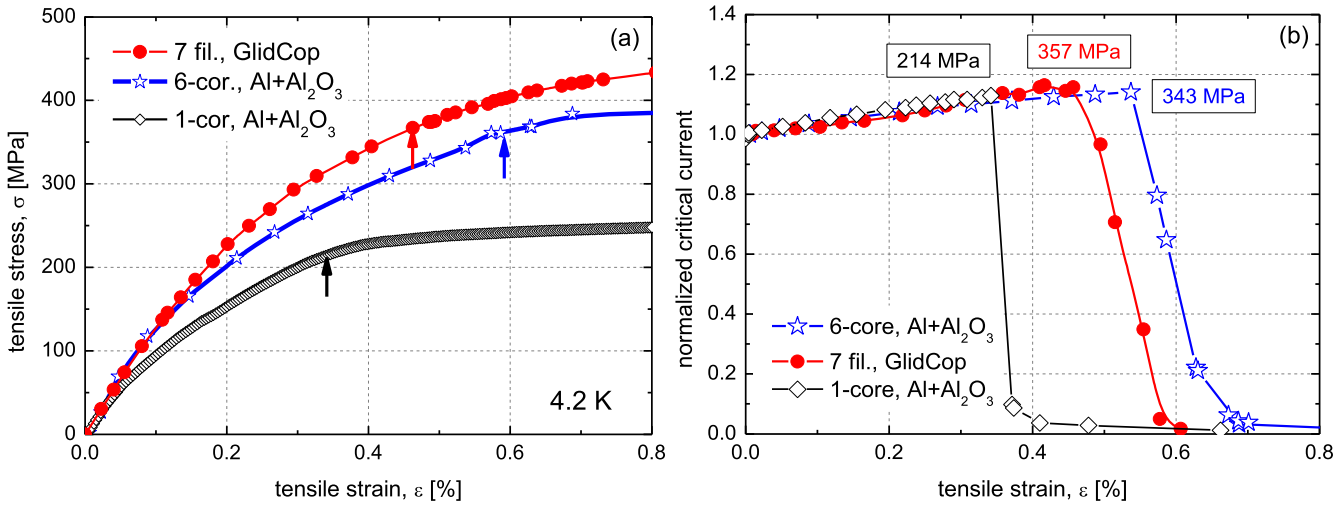


**Figure 7.** Stress–strain characteristics of single- and six-core $Al+Al_2O_3$ sheathed wires in comparison with GlidCop sheathed seven-filament wire (a) and corresponding changes of critical currents with axial strain at 4. 2 K (b).

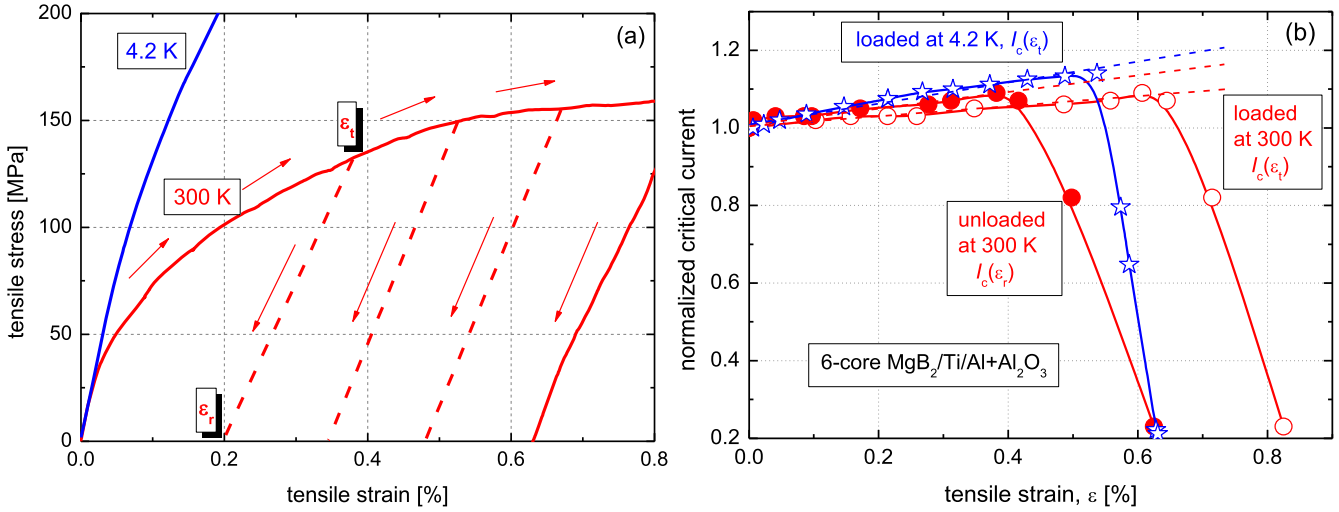


**Figure 8.** Stressing of the six-core wire by tension at room temperature (red curve) compared to $\sigma(\varepsilon)$ at 4.2 K (blue curve) (a) and corresponding normalized critical current versus $\varepsilon$ obtained for loaded tension 4.2 K and 300 K and unloaded tension at 300 K (b).

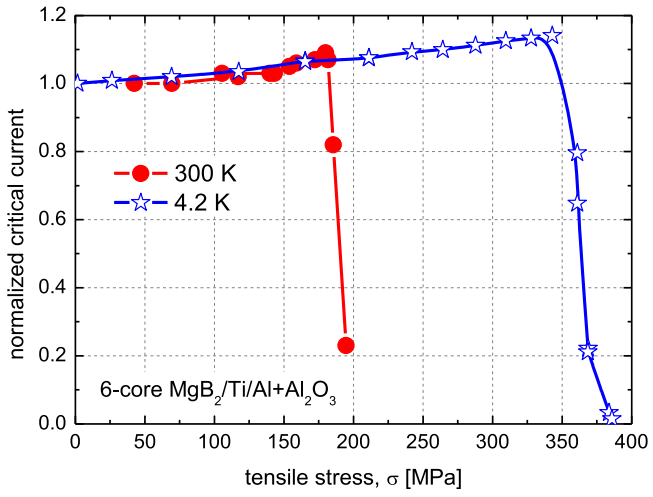


**Figure 9.** Effect of tensile stress applied at 300 K and 4.2 K on the critical current of the six-core $MgB_2/Ti/Al+1.5\%\ Al_2O_3$ wire.

## 4. Conclusions

Filamentary $MgB_2/Ti/Al+Al_2O_3$ superconducting wire combining the lightest composite elements was manufactured by the internal magnesium diffusion into a boron process. Critical current measurements at variable fields, temperatures and the effect of mechanical stresses have shown the following results: (i) an engineering current density of $10^4$ A $cm^{-2}$ is reached at a field of 2 T for 20 K and at 4 T for 5 K. (ii) Current density can be further improved by the densification of boron e.g. applying 2 GPa isostatic pressure, up to 1.5–3.3 times. (iii) Irreversible strain of $Al+Al_2O_3$ sheathed wire $\varepsilon_{irr} = 0.55\%$ and the irreversible stress $\sigma_{irr} = 343$ MPa measured at 4.2 K are very close to those measured for GlidCop sheathed wire ($\varepsilon_{irr} = 0.48\%/\sigma_{irr} = 357$ MPa). (iv) Manipulation stress applied at room temperature is limited to $\sigma_{irr} < 180$ MPa. These properties predetermine the potential use of multi-core $Al+Al_2O_3$ sheathed superconducting wire

for applications where reducing the mass of the system is an important issue.

## Acknowledgments

This work was supported by the Slovak Scientific Agency under the APVV-14-0522 project and the VEGA 2/0129/16 project.

## ORCID iDs

P Kováč https://orcid.org/0000-0003-1872-0359

## References

[1] Park D H, Choi S W, Kim J H and Lee J M 2015 *Cryogenics* **68** 44–58
[2] Marino I, Pujana A, Sarmiento G, Sanz S, Merino J M, Tropeano M, Sun J and Canosa T 2016 *Supercond. Sci. Technol.* **29** 024005
[3] Spillantini P 2010 *Adv. Space Res.* **45** 900–16
[4] Calvelli V, Musenich R, Tunesi F and Battiston R A 2017 *IEEE Trans. Appl. Supercond.* **27** 0500604
[5] Hušek I, Kováč P, Melišek T and Kopera L 2011 *Cryogenics* **51** 550–4
[6] Musenich R, Nardelli D, Brisigotti S, Pietranera D, Tropeano M, Tumino A and Cubeda V 2016 *IEEE Trans. Appl. Supercond.* **26** 6200204
[7] Kováč P, Hušek I, Melišek T, Kulich M, Rosová A, Kováč J, Balog M, Kopera L, Krížik P and Orovčík L 2017 *Supercond. Sci. Technol.* **30** 115001
[8] Kováč P, Hušek I, Rosova A, Kulich M, Kováč J, Melišek T, Kopera L, Balog M and Križik P 2018 *Sci. Rep.* **8** 11229
[9] Balog M, Simančík F, Walcher M, Rajner W and Poletti C 2011 *Mater. Sci. Eng.* A **529** 131–7
[10] Kováč P, Balog M, Hušek I, Kopera L, Križik P, Rosová A, Kováč J, Kulich M and Čaplovičová M 2017 *Cryogenics* **87** 58
[11] Kováč P, Kopera L, Melišek T, Hain M, Kováč J, Kulich M and Hušek I 2018 *Supercond. Sci. Technol.* **31** 015015
[12] Kováč P *et al* 2018 *Supercond. Sci. Technol.* **31** 085003
[13] Kováč P, Hušek I, Melišek T, Kopera L and Kulich M 2016 *Supercond. Sci. Technol.* **29** 10LT01
[14] Kováč P, Hušek I, Kulich M, Melišek T, Kováč J and Kopera L 2016 *Cryogenics* **79** 74–8
[15] Kováč P, Hušek I, Pachla W, Melišek T, Kulich M, Rosova and Kopera L 2016 *Supercond. Sci. Technol.* **29** 075004
[16] Shi Z X, Susner M A, Majoroš M, Sumption M D, Peng X, Rindfleisch M, Tomsic M J and Collings E W 2010 *Supercond. Sci. Technol.* **23** 045018